

Lidar Methods for Observing Mineral Dust

SUGIMOTO Nobuo^{1*} and HUANG Zhongwei² (黄忠伟)

¹ National Institute for Environmental Studies, Tsukuba 305-8506, Japan

² College of Atmospheric Sciences, Lanzhou University, Lanzhou 730000, China

(Received October 12, 2013; in final form January 27, 2014)

ABSTRACT

Lidar methods for observing mineral dust aerosols are reviewed. These methods include Mie scattering lidars, polarization lidars, Raman scattering lidars, high-spectral-resolution lidars, and fluorescence lidars. Some of the lidar systems developed by the authors and the results of the observations and applications are introduced. The largest advantage of the lidar methods is that they can observe vertical distribution of aerosols continuously with high temporal and spatial resolutions. Networks of ground-based lidars provide useful data for understanding the distribution and movement of mineral dust and other aerosols. The lidar network data are actually used for validation and assimilation of dust transport models, which can evaluate emission, transport, and deposition of mineral dust. The lidar methods are also useful for measuring the optical characteristics of aerosols that are essential to assess the radiative effects of aerosols. Evolution of the lidar data analysis methods for aerosol characterization is also reviewed. Observations from space and ground-based networks are two important approaches with the lidar methods in the studies of the effects of mineral dust and other aerosols on climate and the environment. Directions of the researches with lidar methods in the near future are discussed.

Key words: lidar, mineral dust, Mie scattering lidar, Raman lidar, high-spectral-resolution lidar, fluorescence lidar

Citation: Sugimoto Nobuo and Huang Zhongwei, 2014: Lidar methods for observing mineral dust. *J. Meteor. Res.*, **28**(2), 000–000, doi: 10.1007/s13351-014-3068-9.

1. Introduction

Lidars are useful for measuring distribution and optical characteristics of aerosols including mineral dust. In the study of the effects of mineral dust on climate and the environment, it is essential to understand dust emission, transport, deposition, radiative characteristics, and physical and/or chemical characteristics of dust acting as ice and cloud condensation nuclei. They are, however, extremely complicated. Dust emission is dependent on surface conditions such as land cover, soil texture, moisture, vegetation growth, and dynamic condition (e.g., Wang et al., 2008, 2013). The particle size distribution at dust emission is different depending on the source areas and surface conditions. The radiative characteristics of dust are dependent on the chemical composition, size distribution and shape of dust, and they are dif-

ferent depending on source areas (e.g., Bi et al., 2010, 2012). The characteristics of dust can change during transport due to internal mixing with other types of aerosols and/or interaction with gaseous air pollution species (e.g., Qiu and Sun, 1994; Zhou et al., 2002). We may even need to know about bacilli on dust particles in the study of environmental effects.

Lidar methods can provide some essential information that other measurement methods cannot provide. Continuous vertical profile data obtained with even simple Mie scattering polarization lidars are useful for validating dust transport models. Multi-wavelength Raman lidars and/or high-spectral-resolution lidars can provide useful data for characterizing radiative properties that are essential for evaluating the direct and semi-direct effect of mineral dust. Also, they can provide distributions of dust and clouds that can be useful for studying the semi-direct and in-

Supported by the National Natural Science Foundation of China (41205014 and 41375031) and Fundamental Research Funds for the Central Universities (lzujbky-2013-106).

*Corresponding author: nsugimot@nies.go.jp.

direct effect of mineral dust.

Recently, Mona et al. (2012) published a review paper on desert dust characterization with lidars, and an overview of recent studies is presented. In the present paper, we do not intend to provide a comprehensive review of studies of dust using lidars. Instead, we introduce the studies on lidar methods and applications that have been conducted by the authors and discuss the problems and the directions of the future studies.

2. Mie scattering and polarization lidar

2.1 *Mie scattering lidar*

Mie scattering or backscattering is the simplest lidar technique for measuring aerosols and clouds. It transmits laser pulses and receives the backscattered light from aerosols, atmospheric molecules, and clouds. The range to the scatterer is measured by the time of flight of the laser pulse, and the backscattering coefficient is derived from the intensity of the signal. Strictly speaking, however, there is attenuation of the laser in the round-trip path to the scatterer, and the equation describing the lidar signal, so called the lidar equation, contains two unknown parameters, namely, the backscattering coefficient and the extinction coefficient. To solve the lidar equation, we need to make an assumption on the relationship between the backscattering and the extinction coefficients. Therefore, it is sometimes said that Mie scattering lidars cannot make quantitative measurements. It is true that the lidar equation cannot be solved without assumptions, but Mie scattering lidars can provide sufficiently quantitative parameters with reasonable assumptions. Also, we may say that Mie scattering lidars can provide quantitative constraints, for example, to the analysis with chemical transport models.

In the data analysis of Mie scattering lidars, the Fernald's method considering two scattering components (aerosols and molecules) (Fernald, 1984) and the Klett's method considering a single scattering component (Klett, 1981) are usually used. Fernald's method is suitable for optically thin cases. In Fernald's method, the extinction to backscatter ratio (lidar ratio) S_1 is introduced for aerosol scattering. We usu-

ally make an assumption of constant lidar ratio (for example $S_1 = 50$ sr, at 532 nm), however, S_1 is dependent on the types of aerosols. It is about 20 sr for sea salt, and it can be as large as 100 sr for light absorbing aerosols like black carbon. The error in the derived extinction coefficient or the backscattering coefficient due to the error in the assumption of the S_1 value is dependent on the density of observed aerosols (Sasano and Nakane, 1984). In clear conditions, the error in derived backscattering coefficient is small, and the derived backscattering coefficient is not sensitive to the S_1 value. In dense aerosol conditions, the error in the extinction coefficient is smaller. In very dense aerosol cases, Klett's method can provide extinction coefficient profiles quite well. It is sometimes said incorrectly that Mie scattering lidar can measure the backscattering coefficient (not extinction coefficient), but it is approximately correct only in clear conditions. If aerosol optical depth (AOD) is obtained from separate measurements with sun photometers or from the calibrated Mie scattering lidar itself using the Rayleigh scattering signal above the aerosol layer, a method using AOD as a constraint can be used. With such a method, the column averaged S_1 can be determined (Welton et al., 2001).

There are two approaches in pulsed Mie scattering lidars, i.e., the traditional large-pulse-energy low-repetition-rate approach (typically 10 Hz and 100 mJ) (Collis and Russell, 1976) and the small-pulse-energy high-repetition-rate (micro pulse lidar) approach (typically 1 kHz and 1 μ J) (Spinhirne, 1993). Eye-safety is the advantage of the latter approach. There are also continuous wave (CW) lidar methods like random-modulation CW lidar (Takeuchi et al., 1983). However, CW methods generally suffer from the background radiation noise in daytime measurements. Mie scattering lidars are widely used, and there are several commercial lidar systems. Ceilometers are also kinds of Mie scattering lidar.

2.2 *Polarization lidar*

The polarization lidar method is a simple extension of the Mie scattering lidar method adding a polarization analyzer to the receiver. It is extremely useful for detecting non-spherical particles like mineral dust,

because the change in the polarization state by scattering (or the depolarization ratio) is very sensitive to the non-sphericity of the scatterers (Sassen, 1991; Murayama et al., 1999). Usually, a linearly polarized laser beam is transmitted, and parallel and perpendicular polarization components of the received signal are analyzed. We define the depolarization ratio (total depolarization ratio or volume depolarization ratio) by $TDR = P_s/P_p$, where P_p and P_s are the parallel (co-polar) and perpendicular (cross-polar) (“s” stands for German “senkrecht”) polarization components of the received signal. The depolarization ratio can be also defined for the circularly polarized transmitted beam. In commercial micro pulse lidar (MPL4), co-polar component is taken with circularly polarized beam, and cross-polar component is taken with linearly polarized beam. We experimentally compared the linear depolarization ratio derived from an MPL4 and that measured with a linear polarization lidar. The results agreed within the measurement error (Huang et al., 2010).

Because the volume depolarization ratio contains the scattering contribution of Rayleigh scattering of atmospheric molecules, we need to define the particle depolarization ratio (PDR) that represents the depolarization ratio for aerosol scattering. PDR is derived by Eq. (1) (Liu et al., 2002).

$$PDR = \frac{TDR(BR + BR \times MDR - MDR) - MDR}{BR - 1 + BR \times MDR - TDR}, \quad (1)$$

where TDR is the total depolarization ratio, BR is total backscattering to Rayleigh backscattering ratio, and MDR is the depolarization ratio of Rayleigh scattering. MDR is approximately 0.014 (Behrendt and Nakamura, 2002).

We developed a method using the particle depolarization ratio to estimate contributions of non-spherical and spherical aerosols in the extinction coefficient (Sugimoto et al., 2002, 2003; Shimizu et al., 2004). This method is based on the assumption of external mixing of the two types of aerosols, namely mineral dust having a large PDR and spherical aerosols having a small PDR. The contribution of mineral dust in the extinction coefficient (or backscattering coeffi-

cient) is estimated with the following equation.

$$R = \frac{(\delta - \delta_2)(1 + \delta_1)}{(1 + \delta)(\delta_1 - \delta_2)}, \quad (2)$$

where δ is observed PDR, and δ_1 and δ_2 are PDRs of dust and spherical aerosols, respectively. We define the dust extinction coefficient and the spherical aerosol extinction coefficient by multiplying R or $(1-R)$ to the extinction coefficient derived with the Fernald’s or Klett’s method. These methods are useful for analyzing dust and air pollution aerosols in urban area and the down wind regions. The errors caused by the assumed lidar ratio and PDR values were studied by Shimizu et al. (2011), and it was shown that the derived dust extinction coefficient was not sensitive to the assumptions when the density was high. The error is less than 10% in typical dust events.

Figure 1 shows an example of the analysis using this method. In the lidar time-height indications in Fig. 1, distributions of dust and spherical aerosols (air-pollution aerosols) are clearly separated. The number concentrations of particles with diameter larger than 0.4 and 4 μm measured with an optical particle counter are also shown in Fig. 1. It can be seen that there is correlation between the dust extinction coefficient and the number of large particles. In Beijing, heavy air pollution is often observed before dust event as seen in Fig. 1. It is explained by the change in wind direction due to the movement of pressure systems.

2.3 Network of Mie scattering polarization lidars

Networking of Mie scattering polarization lidars is a powerful method for observing three-dimensional distributions and movement of dust and other aerosols. At NIES (National Institute for Environmental Studies), we formed a network of two-wavelength (1064 and 532 nm) Mie scattering and polarization (532 nm) lidars in East Asia in cooperation with other research institutes and universities. The network is named the Asian Dust and aerosol lidar observation Network (AD-Net), and currently 20 lidar stations are operated continuously (<http://www-lidar.nies.go.jp/AD-Net/>). AD-Net is a contributing network to the World Meteorological Organization (WMO) Global Atmosphere

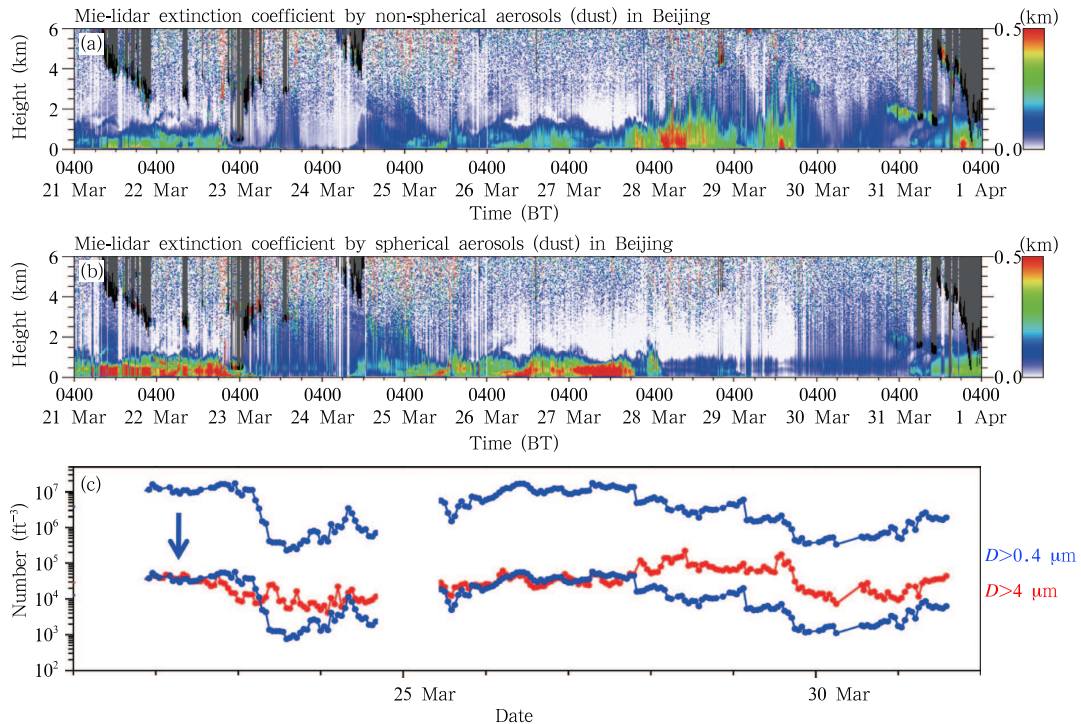


Fig. 1. The extinction coefficient time-height indications at 532 nm for (a) non-spherical aerosols and (b) spherical aerosols derived with the method using the depolarization ratio, compared with (c) the optical particle counter data. Note that the lower blue curve in (c) was shifted from the upper blue one for comparing the temporal variation of number concentration, aiming to show large increases of coarse particles during the dust event (Sugimoto et al., 2008).

Watch (GAW) program. We have developed a real-time data processing system for AD-Net, and can derive the dust and spherical aerosol extinction coefficients at 532 nm as well as the attenuated backscattering coefficients at 532 and 1064 nm and the total depolarization ratio at 532 nm in near realtime (Shimizu et al., 2010).

The data from AD-Net are used in various researches on Asian dust and regional air pollution. One of the important applications of AD-Net data is validation and assimilation of chemical transport models. A four-dimensional variational data assimilation system based on the Chemical weather FORecasting System (CFORS) was developed by Kyushu University with AD-Net dust extinction coefficient data, and analyses of Asian dust events were performed (Uno et al., 2008; Yumimoto et al., 2007, 2008, 2012; Hara et al., 2009; Sugimoto et al., 2010, 2011, 2013). In the data assimilation, a dust emission factor was introduced to control the emission of each grid in the dust source areas. The dust emission factor represents the change

in surface condition that is not considered in the original model. The results of the data assimilation experiments showed that the modeled dust distribution was much improved with the assimilation of AD-Net data. The results also showed that the data assimilation was useful for estimating the amount of dust emission in the source areas. Figure 2 shows an example of assimilated dust extinction coefficient compared with the dust extinction coefficient derived from CALIPSO (see section 5 for annotation). We applied the same data analysis method used for AD-Net to CALIPSO level-1B data to derive the dust and spherical aerosol extinction coefficients. The comparison demonstrated that the model assimilated with AD-Net data reproduced the dust distribution up to far-down wind regions. It was also demonstrated that the data assimilated model reproduced surface PM_{10} data very well. Furthermore, the change in dust emission due to vegetation growth that was not considered in the original model was revealed with the data assimilation (Sugimoto et al., 2010).

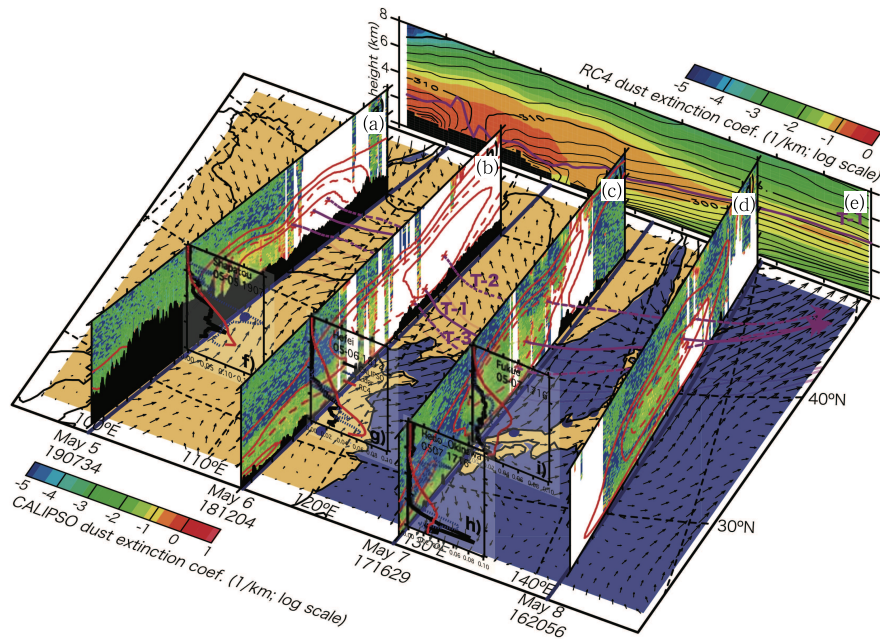


Fig. 2. Dust extinction coefficient calculated with CFORS assimilated with AD-Net data (pink contours) compared with CALIPSO dust extinction coefficient. Lines T-1, T-2, and T-3 are trajectories. Panel (b) indicates dust extinction coefficient profile along trajectory T-1 calculated by the data assimilated CFORS (Uno et al., 2008).

The dust and spherical aerosol extinction coefficient data have also been used in studies of climatology of aerosols in East Asia (Hayasaka et al., 2007; Hara et al., 2011) and in epidemiological studies of the effect of dust aerosols on human health (Kanatani et al., 2010; Kashima et al., 2012; Onishi et al., 2012; Ueda et al., 2012). Using the lidar data in epidemiological studies, we investigated the relationship between the dust and spherical aerosol extinction coefficients and various mass concentration measurements, namely TSP, PM_{10} , SPM, and $PM_{2.5}$. The ratio of mass concentration to the dust extinction coefficient depends on the size distribution of dust, and it changes spatially and temporally. However, there is a high correlation between the dust extinction coefficient and the mass concentration of dust in $PM_{2.5}$ (Sugimoto et al., 2011; Kaneyasu et al., 2012). The relationship between the extinction coefficient and mass concentration is complicated for spherical aerosols because of hygroscopic growth of particles (Sugimoto et al., 2008; Liu et al., 2013). Some of the epidemiological studies (e.g., Onishi et al., 2012) showed that the effect of dust was enhanced when mixed with air pollution aerosols. It

is therefore important to understand mixture state of Asian dust with air pollution aerosols in the future studies.

Studies using a network of lidars were also conducted in arid region (Huang et al., 2008a; Huang et al., 2010). Distribution features of Asian dust in dust events and climatological features such as diurnal variations of dust vertical profile were studied.

3. Raman and high-spectral-resolution lidars

Raman scattering lidars and high-spectral-resolution lidars are techniques for measuring profile of molecular scattering. Since the vertical distribution of atmospheric molecules is known, the extinction coefficient of aerosols can be derived from the attenuation term of the molecular scattering profile (Gao et al., 2009; Wang et al., 2011). In Raman scattering, nitrogen vibrational Raman scattering is usually used for aerosol extinction measurements. In high-spectral-resolution lidars, Rayleigh scattering (strictly speaking, Cabannes scattering) is used (She, 2001). Both Mie scattering and Rayleigh scattering are elas-

tic scattering, and the wavelength of scattered light is the same as the transmitted laser wavelength. However, the spectral width of the scattered light is different. The Rayleigh scattering has much wider Doppler broadening due to the molecular movement in the atmosphere. Consequently, the Mie and Rayleigh scattering components can be separated using a high-resolution spectroscopic element. The technique is called high-spectral-resolution lidar (HSRL). The HSRL method requires a narrow-band laser and a high-resolution spectroscopic element such as an interferometer, but the Rayleigh scattering cross-section is several orders of magnitude higher than Raman scattering. HSRLs are much sensitive compared to Raman lidars, and daytime measurements are possible with relatively small lidar systems (Hua et al., 2004, 2005). The HSRL technique can also be used in space-borne lidars.

With Raman lidar or HSRL methods, the extinction coefficient is obtained independently from the backscattering coefficient. The profile of lidar ratio is consequently determined from the measurement. The lidar ratio is a useful parameter for characterizing aerosols because it is sensitive to the absorption of aerosols (imaginary part of refractive index) and the shape of aerosols. The lidar ratio measurement is also useful for distinguishing aerosols and clouds (Sakai et al., 2003). The extinction and backscattering measurements at multiple wavelengths add independent parameters sufficient for deriving the aerosol microphysical parameters. Müller et al. (2000) developed an inversion method to determine the single scattering albedo, effective radius, etc., from two-wavelength Raman (532 and 355 nm) and three-wavelength Mie (355, 532, and 1064 nm) lidar. The method has been used for characterizing mineral dust aerosols (Müller et al., 2010b, 2013).

At NIES, we constructed an HSRL at 532 nm using an iodine filter as a blocking filter for Mie scattering (Liu et al., 1999) and studied the lidar ratio of Asian dust (Liu et al., 2002). We also added a nitrogen Raman receiver channel to the AD-Net lidars at primary stations (Xie, 2008). Recently, we developed a multi-wavelength HSRL that measures the extinc-

tion coefficient at 2 wavelengths (355 and 532 nm), the backscattering coefficient at 3 wavelengths (355, 532, and 1064 nm), and the depolarization ratio at 2 wavelengths (532 and 1064 nm) (Nishizawa et al., 2012). At the same time, we have developed data analysis methods for the multi-parameter lidars for deriving the concentrations of aerosol components (Nishizawa et al., 2008, 2010). We consider four aerosol components in the analysis of Raman lidars and HSRLs, namely, optically non-absorptive small aerosols (such as sulfate), optically non-absorptive large spherical aerosols (sea salt), non-spherical aerosols (dust), and optically absorptive small aerosols (black carbon). We assume an aerosol optical model for each component (refractive index, size distribution, and shape for dust) and search for the external mixture that best reproduces the observed parameters. In this approach, appropriateness of the definition of the aerosol components and their optical models is essential. The approach is reasonable if the aerosol components are compatible with that used in chemical transport models.

4. Quartz Raman and fluorescence lidars

We observed Raman scattering of quartz in dust particles with a lidar with 532-nm excitation (Tatarov and Sugimoto, 2005). Later measurement was performed at 355 and 532 nm simultaneously, and the Raman scattering signal was confirmed by the wavelength dependence of signal intensity (Müller et al., 2010a).

We also observed fluorescence of aerosols with excitation at 355 nm (Sugimoto et al., 2012a, b). Figure 3 shows examples of fluorescence spectrum. We found that Asian dust were highly fluorescent. It is, however, still not understood what substance (some mineral composition or biological substance on Asian dust) emits fluorescence. We think that it will be useful to compare the fluorescence spectra excited at 266 and 355 nm in the future study for identifying the fluorescent substance. We also found that aerosols transported from urban and industrial areas often emitted fluorescence. We consider that polycyclic aromatic hydrocarbon (PAH) compounds in aerosols emit fluores-

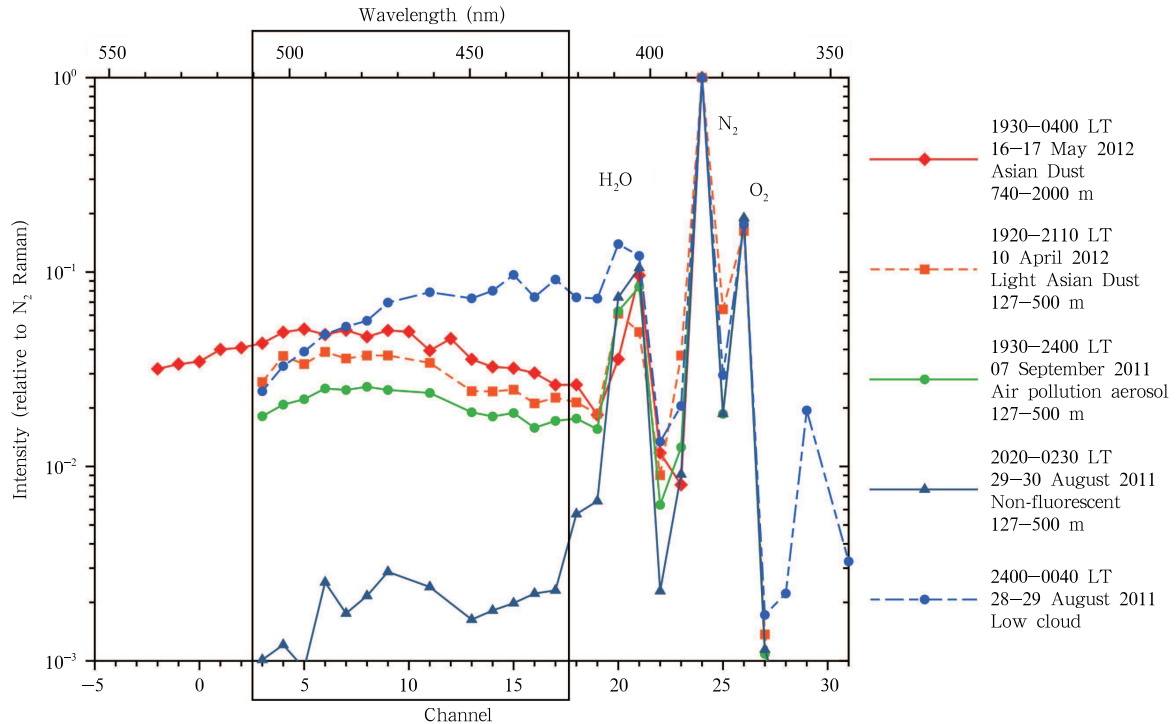


Fig. 3. Examples of the fluorescence spectra for aerosol and clouds (Sugimoto et al., 2012a).

cence. We presented the idea of using the efficiency of broadband fluorescence for characterizing optically absorptive aerosols (Sugimoto et al., 2012a). We also showed that the intensity of the broadband fluorescence was comparable to that of nitrogen vibrational Raman scattering, and a compact lidar system could be used for the broadband fluorescence measurements. The measurement is, however, limited in the nighttime because of solar background radiation.

5. Space-borne lidars

Lidar observations from space are extremely useful for observing aerosols and clouds globally. The first experiment of atmospheric lidar observation from space was LITE (Lidar In-Space Technology Experiment) conducted by U. S. National Aeronautics and Space Administration (NASA) in 1994 using the Space Shuttle. Mie scattering lidar experiments were performed at 3 wavelengths (355, 532, and 1064 nm). Based on the achievement of LITE, lidar satellites GLAS (Geoscience Laser Altimeter System) (launched in 2003) and CALIPSO (Cloud-Aerosol Lidar and In-

frared Pathfinder Satellite Observations) (launched in 2006) were developed. CALIPSO has continued observation normally for more than 7 yr. According to the CALIPSO web site, more than 880 scientific papers using CALIPSO data have been published up to present. A number of studies have been carried out with CALIPSO on mineral dust emission and transport (e.g., Huang et al., 2007; Hara et al., 2008; Liu et al., 2008), optical characteristics of dust (e.g., Zhou et al., 2013), and the effects of mineral dust on radiation and cloud (e.g., Huang et al., 2006, 2010; Xia and Zong, 2009; Wang et al., 2010). Liu et al. (2008) presented a height-resolved global distribution of dust aerosols for the first time based on the first year of CALIPSO lidar measurements under cloud-free conditions. Uno et al. (2009) studied an Asian dust event where dust was transported one full circuit around the globe in 13 days using CALIPSO, ground-based lidars, and a chemical transport model. Sekiyama et al. (2010) reported data assimilation of CALIPSO aerosol data for the first time. Also, there are a number of studies on data analysis method for CALIPSO. Chen et al. (2010), for example, developed dust detection

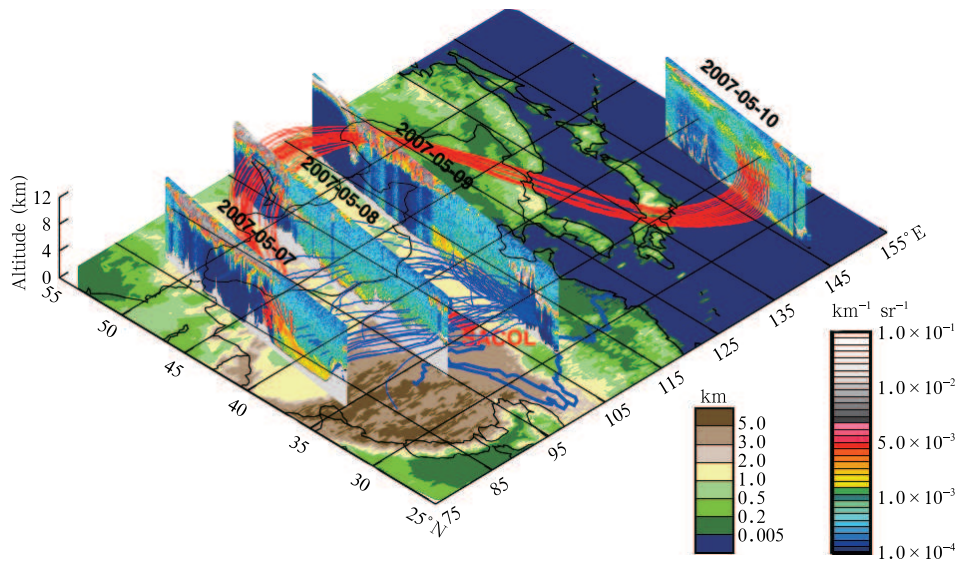


Fig. 4. Examples of long-range transport path of dust aerosols observed by CALIPSO lidar. A dust event that originated in the Taklimakan desert on 7 May 2007 was transported to the Pacific Ocean. Red lines represent back trajectories initialized over the western Pacific; blue lines represent back trajectories initialized over central China. The vertical images (curtain files) show the CALIPSO 532-nm total attenuated backscatter. The color scales on the left represent topographical elevation (Huang et al., 2008b).

algorithm combining the lidar CALIOP (Cloud-Aerosol Lidar with Orthogonal Polarization) and passive IIR (Imaging Infrared Radiometer) on CALIPSO.

Figure 4 shows an example of long-range transport path of dust particles observed by CALIPSO lidar. The result indicates that dust aerosols originated from the Taklimakan desert can also be transported to eastern China through alternative paths (blue lines in Fig. 4). The paths at higher altitudes are dominated by the westerly but the lower-altitude trajectories are determined by regional weather systems and topography.

EarthCARE (Earth Clouds, Aerosols and Radiation Explorer) is being developed jointly by Japan Aerospace Exploration Agency (JAXA) and European Space Agency and planned for launch in 2016. EarthCARE has a lidar named ATLID and a cloud profiling radar (CPR) on the same platform. ATLID is a polarization sensitive 355-nm HSRL. It will provide the extinction coefficient, backscattering coefficient, and depolarization ratio at 355 nm. At NIES, we are developing an aerosol component retrieval algorithm for ATLID based on the same method developed for multi-parameter Raman and high-spectral-resolution lidars

(Nishizawa et al., 2013).

Multi-wavelength HSRL is being studied by NASA for the Aerosol-Cloud-Ecosystems (ACE) mission planned for launch in 2021 (e.g., Hosteler et al., 2012). NASA also plans the Cloud-Aerosol Transport System (CATS) on the International Space Station (McGill et al., 2012). CATS is scheduled for launch in 2014. CATS has three wavelengths and experiments on HSRL are planned at 532 nm. CATS is expected to fill the gap between CALIPSO and ACE.

6. Conclusions

Lidar methods provide essential information for understanding sand dust storm phenomena and their impacts on climate and the environment. Continuous observations of vertical profiles with networks of ground-based lidars provide useful data on emission and transport of mineral dust. Data assimilation of chemical transport model is a powerful method to extract full information from the lidar data. Optical characteristics of dust particles derived from multi-wavelength Raman lidars or HSRLs are useful for estimating radiative effects of mineral dust. Network

observations with multi-parameter lidars can be useful for studying the changes in characteristics of mineral dust during transport. Lidar methods like fluorescence lidar can provide additional information on composition of dust and biological substance on dust particles.

Internal mixing of dust and other aerosols is important both in the radiative effects and the effects on the environment and human health. Reliable optical models that describe the optical characteristics of mineral dust and internally mixed mineral dust are essential for data analysis of multi-parameter lidars and for the calculation of radiative effects. The experimental studies combining multi-parameter lidars, in-situ instruments, and chemical and microscopic analyses with aerosol sampling will be needed to understand the phenomena and to make such optical models. At the same time, the studies on handling internal mixture in chemical transport models are required. Advances in chemical transport models and lidar data analysis methods should be closely linked. We expect that they will merge in data assimilation in the future.

Acknowledgments. We would like to thank Dr. Jianping Huang at Lanzhou University for discussions and critical reading of the manuscript.

REFERENCES

- Bi, J. R., J. P. Huang, Q. Fu, et al., 2010: Toward characterization of the aerosol optical properties over Loess Plateau of northwestern China. *J. Quant. Spectrosc. Radiat. Transf.*, **112**, 346–360.
- , —, —, et al., 2012: Field measurement of clear-sky solar irradiance in Badain Jaran Desert of northwestern China. *J. Quant. Spectrosc. Radiat. Transf.*, **122**, 194–207.
- Behrendt, A., and T. Nakamura, 2002: Calculation of the calibration constant of polarization lidar and its dependency on atmospheric temperature. *Opt. Express*, **10**, 805–817.
- Chen, B., J. Huang, P. Minnis, et al., 2010: Detection of dust aerosol by combining CALIPSO active lidar and passive IIR measurements. *Atmos. Chem. Phys.*, **10**, 4241–4251.
- Collis, R. T. H., and P. B. Russell, 1976: Lidar measurement of particles and gases by elastic backscattering and differential absorption. *Laser Monitoring of the Atmosphere, Topics in Applied Physics*, **14**, 71–151.
- Fernald, F. G., 1984: Analysis of atmospheric lidar observations: Some comments. *Appl. Opt.*, **23**, 652–653.
- Gao Fei, Song Xiaoquan, Wang Yufeng, et al., 2009: Ultraviolet Raman lidar for high accurate profiling of aerosol extinction coefficient. *Chinese Opt. Lett.*, **7**, 95–97.
- Hara, Y., I. Uno, K. Yumimoto, et al., 2008: Summer-time Taklimakan dust structure. *Geophys. Res. Lett.*, **35**, L23801, doi: 10.1029/2008GL035630.
- , K. Yumimoto, I. Uno, et al., 2009: Asian dust outflow in the PBL and free atmosphere retrieved by NASA CALIPSO and an assimilated dust transport model. *Atmos. Chem. Phys.*, **9**, 1227–1239.
- , I. Uno, A. Shimizu, et al., 2011: Seasonal characteristics of spherical aerosol distribution in eastern Asia: Integrated analysis using ground/space-based lidars and a chemical transport model. *SOLA*, **7**, 121–124, doi: 10.2151/sola.2011-031.
- Hayasaka, T., S. Satake, A. Shimizu, et al., 2007: Vertical distribution and optical properties of aerosols observed over Japan during ABC-EAREX2005. *J. Geophys. Res.*, **112**, D22S35, doi: 10.1029/2006JD008086.
- Hosteler, C. A., R. A. Ferrare, J. W. Hair, et al., 2012: Airborne multi-wavelength high spectral resolution lidar for process studies and assessment of future satellite remote sensing. AGU Fall Meeting, A13K-0336.
- Hua, D., M. Uchida, and T. Kobayashi, 2004: Ultraviolet high-spectral-resolution Rayleigh-Mie lidar with a dual-pass Fabry-Perot etalon for measuring atmospheric temperature profiles of the troposphere. *Opt. Lett.*, **29**, 1063–1065.
- , —, and —, 2005: UV Rayleigh-Mie lidar for daytime temperature profiling of the troposphere. *Appl. Opt.*, **44**, 1315–1322.
- Huang, J. P., B. Lin, P. Minnis, et al., 2006: Satellite-based assessment of possible dust aerosols semi-direct effect on cloud water path over East Asia. *Geophys. Res. Lett.*, **33**, doi: 10.1029/2006GL026561.
- , P. Minnis, Y. H. Yi, et al., 2007: Summer dust aerosols detected from CALIPSO over the Tibetan Plateau. *Geophys. Res. Lett.*, **34**, L18805, doi: 10.1029/2007GL029938.
- , Zhang Wu, Zuo Jinqing, et al., 2008a: An overview of the semi-arid climate and environment research

- observatory over the Loess Plateau. *Adv. Atmos. Sci.*, **25**, 906–921.
- , P. Minnis, B. Chen, et al., 2008b: Long-range transport and vertical structure of Asian dust from CALIPSO and surface measurements during PACDEX. *J. Geophys. Res.*, **113**, D23212, doi: 10.1029/2008JD010620.
- , —, H. Yan, et al., 2010: Dust aerosol effect on semi-arid climate over Northwest China detected from A-Train satellite measurements. *Atmos. Chem. Phys.*, **10**, 6863–6872.
- Huang, Z. W., N. Sugimoto, J. Huang, et al., 2010: Comparison of depolarization ratio measurements with micro-pulse lidar and a linear polarization lidar in Lanzhou, China. Proc. 25th Int. Laser Radar Conf., St. Petersburg, Russia, 528–531.
- , J. P. Huang, J. R. Bi, et al., 2010c: Dust aerosol vertical structure measurements using three MPL lidars during 2008 China–U.S. joint dust field experiment. *J. Geophys. Res.*, **115**, D00K15, doi: 10.1029/2009JD013273.
- Kanatani, K. T., I. Ito, W. K. Al-Delaimy, et al., 2010: Desert-dust exposure is associated with increased risk of Asthma hospitalization in children. *Am. J. Respir. Crit. Care Med.*, **182**, 1475–1481, doi: 10.1164/rccm.201002-0296OC.
- Kaneyasu, N., N. Sugimoto, A. Shimizu, et al., 2012: Comparison of lidar-derived dust extinction coefficients and the mass concentrations of surface aerosol. *J. Japan. Soc. Atmos. Environ.*, **47**, 285–291. (in Japanese)
- Kashima, S., T. Yorifuji, T. Tsuda, et al., 2012: Asian dust and daily all-cause or cause-specific mortality in western Japan. *Occup. Environ. Med.*, **69**, 908–915, doi: 10.1136/oemed-2012-100797.
- Klett, J. D., 1981: Stable analytical inversion solution for processing lidar returns. *Appl. Opt.*, **20**, 211–220.
- Liu Dong, Wang Zhien, Liu Zhaoyan, et al., 2008: A height resolved global view of dust aerosols from the first year CALIPSO lidar measurements. *J. Geophys. Res.*, **113**(D16), doi: 10.1029/2007JD009776.
- Liu, X. G., J. Li, Y. Qu, et al., 2013: Formation and evolution mechanism of regional haze: A case study in the megacity Beijing, China. *Atmos. Chem. Phys.*, **13**, 4501–4514, doi: 10.5194/acp-13-4501-2013.
- Liu, Z. Y., I. Matsui, and N. Sugimoto, 1999: High-Spectral-Resolution lidar using an iodine absorption filter for atmospheric measurements. *Opt. Engineering*, **38**, 1661–1670.
- , N. Sugimoto, and T. Murayama, 2002: Extinction-to-backscatter ratio of Asian dust observed by high-spectral-resolution lidar and Raman lidar. *Appl. Opt.*, **41**, 2760–2767.
- , D. Liu, J. Huang, et al., 2008: Airborne dust distributions over the Tibetan Plateau and surrounding areas derived from the first year of CALIPSO lidar observations. *Atmos. Chem. Phys.*, **8**, 5045–5060.
- McGill, M., E. Welton, J. Yorks, et al., 2012: CATS: A new earth science capability. *The Earth Observer*, **24**, 4–8.
- Mona, L., Z. Liu, D. Müller, et al., 2012: Lidar measurements for desert dust characterization: An overview. *Adv. Meteor.*, doi: 10.1155/2012/356265.
- Müller, D., U. Wandinger, and A. Ansmann, 2000: Microphysical particle parameters from extinction and backscatter lidar data by inversion with regularization: Experiment. *Appl. Opt.*, **39**, 1879–1892.
- , I. Mattis, B. Tatarov, et al., 2010a: Mineral quartz concentration measurements of mixed mineral dust/urban haze pollution plumes over Korea with multiwavelength aerosol Raman-quartz lidar. *Geophys. Res. Lett.*, **37**, L20810, doi: 10.1029/2010GL044633.
- , A. Ansmann, V. Freudenthaler, et al., 2010b: Mineral dust observed with AERONET Sun photometer, Raman lidar, and in-situ measurements during SAMUM 2006: Shape-dependent particle properties. *J. Geophys. Res.*, **115**, D11207, doi: 10.1029/2009JD012523
- , I. Veselovskii, A. Kolgotin, et al., 2013: Vertical profiles of pure dust and mixed smoke-dust plumes inferred from inversion of multiwavelength Raman/polarization lidar data and comparison to AERONET retrievals and in-situ observations. *Appl. Opt.*, **52**, 3178–3202.
- Murayama, T., H. Okamoto, N. Kaneyasu, et al., 1999: Application of lidar depolarization measurement in the atmospheric boundary layer: Effects of dust and sea-salt particles. *J. Geophys. Res.*, **104**, 31781–31792.
- Nishizawa, T., N. Sugimoto, I. Matsui, et al., 2008: Algorithm to retrieve aerosol optical properties from high-spectral-resolution lidar and polarization Mie-scattering lidar measurements. *IEEE Trans. Geosci. Rem. Sens.*, **46**, 4094–4103.

- , —, —, et al., 2010: Algorithms to retrieve optical properties of three-component aerosols from two-wavelength backscatter and one-wavelength polarization lidar measurements considering nonsphericity of dust. *J. Quant. Spectrosc. Radiat. Transf.*, **112**, 254–267, doi: 10.1016/j.jqsrt.2010.06.002.
- , N. Sugimoto, I. Matsui, et al., 2012: Development of two-wavelength high-spectral-resolution lidar and application to shipborne measurements. Proc. 26th Int. Laser Radar Conf., Porto Heli, Greece.
- , A. Higurashi, N. Sugimoto, et al., 2013: Development of aerosol and cloud retrieval algorithms using ATLID and MSI data of EarthCARE. *AIP Conf. Proc.*, **1531**, 472, doi: 10.1063/1.4804809.
- Onishi, K., S. Kurosaki, S. Otani, et al., 2012: Atmospheric transport route determines components of Asian dust and health effects in Japan. *Atmospheric Environment*, **49**, 94–102, doi: 10.1016/j.atmosenv.2011.12.018.
- Qiu Jinhuan and Sun Jinhui, 1994: Optically remote sensing of the dust storm and results analysis. *Chinese J. Atmos. Sci.*, **18**, 1–10, doi: 10.3878/j.issn.1006-9895. (in Chinese)
- Sakai, T., T. Nagai, M. Nakazato, et al., 2003: Ice clouds and Asian dust studied with lidar measurements of particle extinction-to-backscatter ratio, particle depolarization, and water-vapor mixing ratio over Tsukuba. *Appl. Opt.*, **42**, 7103–7116.
- Sasano, Y., and H. Nakane, 1984: Significance of the extinction/backscatter ratio and the boundary value term in the solution for the two-component lidar equation. *Appl. Opt.*, **23**, 11–13.
- Sassen, K., 1991: The polarization lidar technique for cloud research: A review and current assessment. *Bull. Amer. Meteor. Soc.*, **72**, 1848–1866.
- Sekiyaama, T. T., T. Y. Tanaka, A. Shimizu, et al., 2010: Data assimilation of CALIPSO aerosol observations. *Atmos. Chem. Phys.*, **10**, 39–49.
- She, C. Y., 2001: Spectral structure of laser light scattering revisited. Band widths of nonresonant scattering lidars. *Appl. Opt.*, **40**, 4875–4884.
- Shimizu, A., N. Sugimoto, I. Matsui, et al., 2004: Continuous observations of Asian dust and other aerosols by polarization lidar in China and Japan during ACE-Asia. *J. Geophys. Res.*, **109**, D19S17, doi: 10.1029/2002JD003253.
- Shimizu, A., N. Sugimoto, and I. Matsui, 2010: Detailed description of data processing system for lidar network in East Asia. Proc. 25th Int. Laser Radar Conf. St. Petersburg, Russia, 911–913.
- , —, —, et al., 2011: Relationship between Lidar-derived dust extinction coefficients and mass concentrations in Japan. *SOLA*, **7A**, 1–4.
- Spinhirne, J. D., 1993: Micro pulse lidar. *IEEE Trans. Geosci. Rem. Sens.*, **31**, 48–55.
- Sugimoto, N., I. Matsui, A. Shimizu, et al., 2002: Observation of dust and anthropogenic aerosol plumes in the Northwest Pacific with a two-wavelength polarization lidar on board the research vessel Mirai. *Geophys. Res. Lett.*, **29**, doi: 10.1029/2002GL015112.
- , I. Uno, M. Nishikawa, et al., 2003: Record heavy Asian dust in Beijing in 2002: Observations and model analysis of recent events. *Geophys. Res. Lett.*, **30**, 1640, doi: 10.1029/2002GL016349.
- , I. Matsui, A. Shimizu, et al., 2008: Lidar network observations of tropospheric aerosols. *Proc. SPIE*, **7860**, 71530A, doi: 10.1117/12.806540.
- , Y. Hara, K. Yumimoto, et al., 2010: Dust emission estimated with an assimilated dust transport model using lidar network data and vegetation growth in the Gobi desert in Mongolia. *SOLA*, **6**, 125–128, doi: 10.2151/sola.2010-032.
- , Y. Hara, A. Shimizu, et al., 2011: Comparison of surface observations and a regional dust transport model assimilated with lidar network data in Asian dust event of March 29 to April 2, 2007. *SOLA* **7A**, 013–016, doi:10.2151/sola.7A-004.
- , Z. Huang, T. Nishizawa, et al., 2012a: Fluorescence from atmospheric aerosols observed with a multi-channel lidar spectrometer. *Opt. Express*, **20**, 20800–20807, doi: 10.1364/OE.20.020800.
- , —, —, et al., 2012b: Study of fluorescence of atmospheric aerosols using a lidar spectrometer. *Proc. of SPIE*, **8526**, 852607, doi: 10.1117/12.977177.
- , Y. Hara, A. Shimizu, et al., 2013: Analysis of dust events in 2008 and 2009 using the lidar network, surface observations and the CFORS model. *Asia-Pacific J. Atmos. Sci.*, **49**, 27–39.
- Takeuchi, N., N. Sugimoto, H. Baba, et al., 1983: Random modulation CW lidar. *Appl. Opt.*, **22**, 1382–1386.
- Tatarov, B., and N. Sugimoto, 2005: Estimation of quartz concentration in the tropospheric mineral aerosols using combined Raman and high-spectral-resolution lidars. *Opt. Lett.*, **30**, 3407–3409.
- Ueda, K., A. Shimizu, H. Nitta, et al., 2012: Long-range transported Asian Dust and emergency ambulance dispatches. *Inhal. Toxicol.*, **24**, 858–867, doi: 10.3109/08958378.2012.724729.

- Uno, I., K. Yumimoto, A. Shimizu, et al., 2008: 3D structure of Asian dust transport revealed by CALIPSO and a 4DVAR dust model. *Geophys. Res. Lett.*, **35**, L06803, doi: 10.1029/2007GL032329.
- , K. Eguchi, K. Yumimoto, et al., 2009: Asian dust transported one full circuit around the globe. *Nature Geosci.*, **2**, doi: 10.1038/NGEO583.
- Wang, W. C., J. P. Huang, P. Minnis, et al., 2010: Dusty cloud properties and radiative forcing over dust source and downwind regions derived from A-Train data during the Pacific Dust Experiment. *J. Geophys. Res.*, **115**, doi: 10.1029/2010JD014109.
- Wang, X., S. J. Doherty, and J. P. Huang, 2013: Black carbon and other light-absorbing impurities in snow across northern China. *J. Geophys. Res.-Atmos.*, **118**, 1471–1492, doi: 10.1029/2012jd018291.
- Wang, X., J. P. Huang, M. X. Ji, et al., 2008: Variability of East Asian dust events and their long-term trend. *Atmos. Environ.*, **42**, 3156–3165, doi: 10.1016/j.atmosenv.2007.07.046.
- Wang, Y. F., D. X. Hua, J. D. Mao, et al., 2011: A detection of atmospheric relative humidity profile by UV Raman lidar. *J. Quant. Spectrosc. Radiat. Transf.*, **112**, 214–219, doi: 10.1016/j.jqsrt.
- Welton, E. J., J. R. Campbell, J. D. Spinhirne, et al., 2001: Global monitoring of clouds and aerosols using a network of micro-pulse lidar systems. *Proc. SPIE*, **4153**, 151–158.
- Yumimoto, K., I. Uno, N. Sugimoto, et al., 2007: Adjoint inverse modeling of dust emission and transport over East Asia. *Geophys. Res. Lett.*, **34**, L08806, doi: 10.1029/2006GL028551.
- , —, —, et al., 2008: Adjoint inversion modeling of Asian dust emission using lidar observations. *Atmos. Chem. Phys.*, **8**, 2869–2884.
- , —, —, et al., 2012: Size-resolved adjoint inversion of Asian dust. *Geophys. Res. Lett.*, **39**, L24807, doi: 10.1029/2012GL053890.
- Zhou, J., G. M. Yu, C. J. Jin, et al., 2002: Lidar observations of Asian Dust over Hefei, China, in Spring of 2000. *J. Geophys. Res.*, **107**, doi: 10.1029/2001JD000802.
- Zhou, T., J. P. Huang, Z. W. Huang, et al., 2013: The depolarization-attenuated backscatter relationship for dust plumes. *Opt. Express*, **21**, 15195–15204, doi: 10.1364/OE.21.015195.
- Xia, X. A., and X. M. Zong, 2009: Shortwave versus longwave direct radiative forcing by Taklimakan dust aerosols. *Geophys. Res. Lett.*, **36**, L07803, doi: 10.1029/2009GL037237.
- Xie, C. B., T. Nishizawa, N. Sugimoto, et al., 2008: Characteristics of aerosol optical properties in pollution and Asian dust episodes over Beijing, China. *Appl. Opt.*, **47**, 4945–4951.